Geometric Structures Using Model Predictive Control for an Electromagnetic Actuator

Paolo Mercorelli
Leuphana University of Lueneburg
Institute of Product and Process Innovation
Volgershall 1, D-21339 Lueneburg
Germany
mercorelli@uni.leuphana.de

Abstract: Control of permanent magnetic actuators is not an easy task because of the presence of the nonlinear quadratic terms of the currents. In order to achieve a suitable controlled dynamics canceling the effect of the nonlinearity, a new control strategy has been conceived. The proposed strategy combines the geometric eigenvector concept through a pre-compensation action and a Model Predictive Control (MPC) strategy. The pre-compensation action is conceived through an input partition matrix based on the eigenvector concept. It is known that each eigenvector represents an invariant subspace for the system and this property is useful to realize a very simple control technique which is able to speed up the controlled dynamics without incurring oscillations. This technique can be applied to a large variety of actuators. Simulation results are reported to validate the proposed strategy.

Key–Words: Geometric control, Linear control, Model predictive control

1 Introduction and motivations

In the past three decades, research on the geometric approach to dynamic systems theory and control has allowed the development of instruments and has become a powerful and a thorough tool for the analysis and synthesis of dynamic systems [1], [2], [3]. Over the same time period, mechanical systems used in industry and developed in research labs have also evolved rapidly. Interests in robust control by using geometric approach have been developed during the last few years [4, 5, 6]. Recently, the interest in this topic has increased in theoretical aspects and applications as well, see for instance [7, 8], particulary on problems like non-interaction and noise localization, see [9]. As an important mechatronic component, electromagnetic actuators are used in many industrial applications, in particular in automotive and production systems. In production systems they are used for movements and precise positioning. Mechanical or hydraulic-mechanical components have been replaced by electromagnetic actuators due to their high efficiency, excellent dynamic behavior and small size. Generally, there is a large variety of different electromagnetic actuators for motions. For long strokes, AC linear motor concepts are often preferred while for micro and nanometer applications special designs based on piezoelectric or magnetostrictive principles have been frequently investigated. However, for moving distances between 5 and 15 mm, DC linear motors (especially using permanent magnets as excitation) have been proven to be advantageous in industrial applications. Particular applications using electromagnetic actuators are presented in [10], [11], and [12] in which different kinds of actuators are used to generate movement of valves for engine applications. Linear actuators play a very important role in conceiving new mechanisms and applications in the actuator theory field. This paper proposes a method based on a geometric approach which, moreover, involves the concept of the eigenvectors generating a very simple controller structure. The idea consists of using eigenvectors as structural invariant subspaces to preselect a suitable controlled subspace. To show the effectiveness of this approach, the paper considers using a position controller for a linear electromagnetic actuator used for industrial applications to move a mass with a high precision. A controller based on a controlled invariant subspace cancels the current nonlinearity. The presented actuator can be described by using four state variables. The system is nonlinear and time varying. In particular, the nonlinearities consist of quadratic current terms $i_1^2(t) - i_2^2(t)$ and nonlinear induced voltages $u_q(t)$. Because of the special form of the current nonlinearity it is possible to eliminate, or at least to reduce the nonlinearity by using a controller based on a controlled invariant subspace. In [13] the authors considered the same problem, and they proposed a solution based on the decoupling and thus considered transforming two controlled invariant subspaces into two constrained controlled invariant subspaces. Therefore the proposed method in [14] represents an enhancement of that proposed in [13] realizing a very simple controller structure which is based on the idea of transforming a unique controlled invariant subspace into an invariant one. This paper considers the results presented in [13] and improves them using the eigenvectors of the matrix describing the dynamics of the actuator. A pre-compensation control structure, which is able to speed up the controlled output without incurring oscillations of the controlled output, is considered. In drive and actuator systems as well as in electrical machines the nonlinearities play a crucial role in the design of the controller. In practical applications, to achieve stability and moreover an acceptable ratio of convergence of a tracking problem, complex control structures are often the result from the controller analysis design. The idea is to utilize the linear prediction algorithm to obtain the tracking. However, the computation burden in solving the optimization problem on-line usually limits the MPC applications by slow dynamic systems [15]. Recently the study of applying MPC to mechatronic systems for servo design draws much interest from many researchers, owing to the emerging development of microprocessor technology, as in [16] and also in different fields of the control engineering as in [17], [18] and [19]. Moreover, various advanced techniques integrating with MPC for performance improvement [20], have also rapidly developed. The two control structures, geometric controller and MPC are organised in a cascade form. The resulting controller can be seen as a two stage controller in which the first stage consists of a geometric control law which cancels the nonlinearity of the electrical system. In the second stage of the control structure, an MPC is used to predict the output to be tracked. The advantage of this combination consists of an improvement of the dynamic performances, as shown by the computer simulations, and in the mean time, by using a geometric controller in the first stage of the control structure a linearising action is performed. Therefore a linear MPC is applicable with its exact off-line optimal solution and an On-line optimisation problem can be avoided. The paper is organized in the following way. Section 2 is devoted to the model description. Section 3 shows the problem statement. Section 4 shows a possible procedure to cancel the nonlinearity in the actuator and presents the procedure which uses the eigenvectors and eigenvalues to speed up the dynamics of the whole actuator using a pre-controller structure. Section 5 shows a Model Predictive Controller (MPC) which represents the main regulator of the actuator. The simulation results and conclusions close the paper.

The main nomenclature

$\mathbf{u}_{in}(t)$: input voltage vector
$\mathbf{i}(t)$: coil current vector
$x(t)$: position of the armature
$\dot{x}(t) = v(t)$: velocity of the armature
$\mathbf{u}_q(t)$: induced voltage vector
R_c: coil resistance
L_c: coil inductance
$\mathbf{B}_g$: magnetic flux density vector
Θ_M: magnetic voltage sources of the permanent magnets
$\Theta_{Coil} = \Theta_{Coil1} + \Theta_{Coil2}$: magnetic voltage source of both coils
$F_L(t)$: Lorentz force
$F_0(t)$: disturbance force
$\mathbf{A}$: state matrix of the electrical model
$\mathbf{B}$: input matrix of the electrical model
$\mathscr{B} = \mathrm{im}\mathbf{B}$: image of matrix $\mathbf{B}$
(subspace spanned by the columns of matrix $\mathbf{B}$)
$\mathbf{A}_w$: state matrix of the whole actuator linearized model
$\mathbf{B}_w$: input matrix of the whole actuator linearized model
$\mathscr{B}_w = \mathrm{im}\mathbf{B}_w$: image of matrix $\mathbf{B}_w$
(subspace spanned by the columns of matrix $\mathbf{B}_w$)
$\mathbf{V}_w$: eigenvectors of matrix $\mathbf{A}_w$
$\min\mathscr{I}(\mathbf{A}, \mathscr{B}) = \sum_{i=0}^{n-1} \mathbf{A}^i \mathrm{im}\mathbf{B}$: minimum $\mathbf{A}$–invariant subspace containing $\mathrm{im}(\mathbf{B})$
$\mathbf{F}$: decoupling feedback gain matrix
$\mathbf{S}_i$: decoupling input partition matrix with $i = 1, 2$.
$\mathscr{S}_i = \mathrm{im}\mathbf{S}_i$: image of matrix $\mathbf{S}_i$ with $i = 1, 2$.
(subspace spanned by the columns of matrix $\mathbf{S}_i$)
$\mathbf{S}_p$: eigenvector input partition matrix
$\mathscr{S}_p = \mathrm{im}\mathbf{S}_p$: image of matrix $\mathbf{S}_p$
(subspace spanned by the columns of matrix $\mathbf{S}_p$)
$\mathscr{I}$: invariant subspace
$\mathbf{I}_i$: currents matrix with $i = 1, 2$.
$\mathscr{C}_i$: image of the current subspaces with $i = 1, 2$.
$\mathscr{R}_{I_i}$: minimum current invariant subspace with $i = 1, 2$.
$\mathbf{x}_f$: discrete state vector
$\mathbf{A}_{wk}$: discrete state matrix of the whole actuator linearized model
$\mathbf{B}_{wk}$: discrete input matrix of the whole actuator linearized model

2 Model description

The geometry of the considered linear motor is given in Fig. 1. The device consists of an outer and an inner iron part. Permanent magnets are mounted on top of the inner iron bar. Their polarization is indicated by the element arrows. The actuator's coils are attached to the outer iron. Each coil is equipped with a separate voltage input. For controller design purposes the dynamical model of the linear motor must be identified.

2.1 The electrical system

Figure 2 demonstrates the equivalent electrical circuit diagram of the actuator's coils. The electrical system

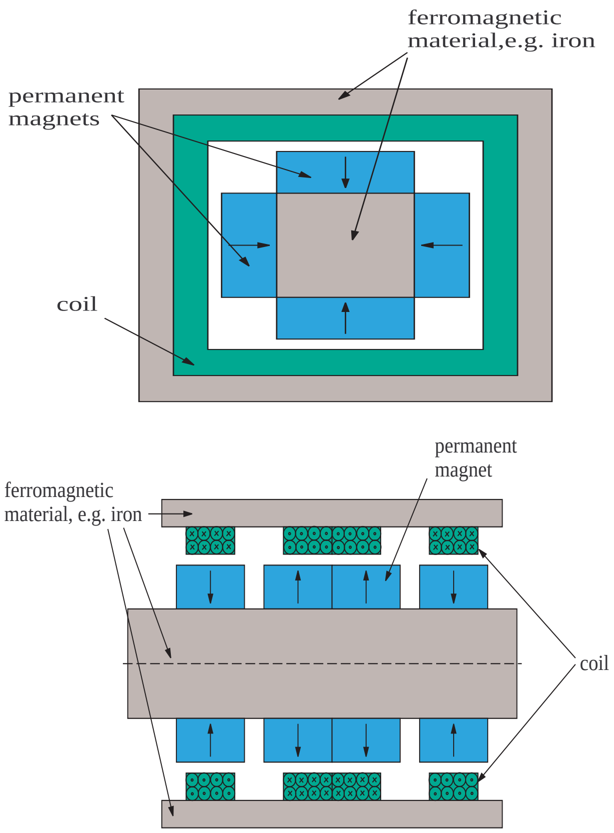

Figure 1: Geometry of the actuator, front (top) and side section (bottom).

of the coils is generally given by:

$$\mathbf{u}_{in}(t) = R_c\mathbf{i}(t) + L_c\frac{d\mathbf{i}(t)}{dt} + \mathbf{u}_q(t),$$

where $\mathbf{u}_{in}(t)$ represents the input voltage vector, $\mathbf{i}$ represents the coil current vector and R_c and L_c the resistance and the inductance of the coil windings. The induced voltages $\mathbf{u}_q(t) = lv(t)\mathbf{B}_g$ are generated due to the armature speed $v(t)$. Parameter l represents the

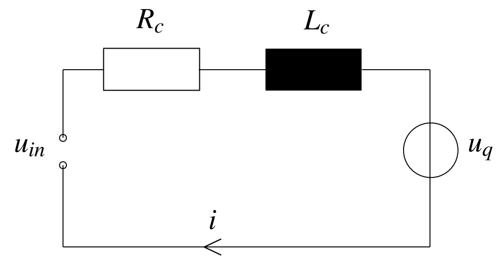

Figure 2: Equivalent electrical circuit diagram.

coil length and $\mathbf{B}_g$ represents the magnetic flux density vector in the air gap. From Fig. 1 it is easy to see that:

$$\mathbf{B}_g = \begin{bmatrix} B_{g1} & B_{g2} \end{bmatrix}^T,$$

where $B_{g1} = -B_{g2}$. A vectorial expression of the induced voltage is not required since the geometry boundaries are quadratical, see Fig. 1. Finite-element simulations prove that considering a quarter of the geometry is sufficient for modeling the magnetic system of the actuator (see Fig. 3). Thus, taking into account all self and coupling inductances and reducing the geometry only to two coils (quarter of geometry), the electrical system of Eq. (1) can be derived:

$$\begin{bmatrix} \frac{di_1(t)}{dt} \\ \frac{di_2(t)}{dt} \end{bmatrix} = \begin{bmatrix} -\frac{R_c}{L_{c1}L_{c5}} & \frac{R_cL_{c2}}{L_{c1}L_{c3}L_{c5}} \\ \frac{R_cL_{c4}}{L_{c1}L_{c3}L_{c5}} & -\frac{R_c}{L_{c3}L_{c5}} \end{bmatrix} \begin{bmatrix} i_1(t) \\ i_2(t) \end{bmatrix} + \begin{bmatrix} \frac{1}{L_{c1}L_{c5}} & -\frac{L_{c2}}{L_{c1}L_{c3}L_{c5}} \\ -\frac{L_{c4}}{L_{c1}L_{c3}L_{c5}} & \frac{1}{L_{c3}L_{c5}} \end{bmatrix} \begin{bmatrix} u_{in1}(t) - u_{q_1}(t) \\ u_{in2}(t) - u_{q_2}(t) \end{bmatrix}, \tag{1}$$

with

$$L_{c1} = L_{11} + L_{41}; \quad L_{c2} = L_{21} + L_{31}$$
$$L_{c3} = L_{22} + L_{32}; \quad L_{c4} = L_{12} + L_{42}$$
$$L_{c5} = 1 - \frac{L_{c2}L_{c4}}{L_{c1}L_{c3}}, \tag{2}$$

where L_{11} and L_{12} are the self-inductances of coil 1 and coil 2. The remaining inductances in Eqs. (2) represent the coupled inductances among the coils.

2.2 The magnetic system

Figure 3 represents the reduced, quarter geometry as well as its equivalent magnetic circuit diagram (compare with geometry, Fig. 1). The expressions Θ_M and

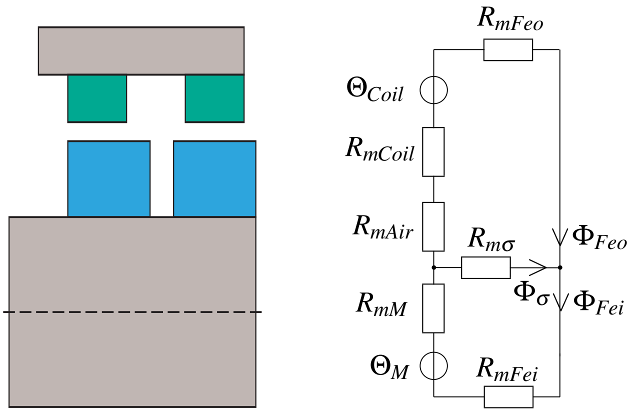

Figure 3: Quarter of the geometry and equivalent magnetic circuit diagram.

Θ_{Coil} represent the magnetic voltage sources of the permanent magnets and the coils. The magnetic resistances of the air gap, the iron parts, the coil and the permanent magnets are expressed by term R_m. The magnetic flux through the equivalent elements is represented by Φ. The element $\Theta_{Coil} = \Theta_{Coil1} + \Theta_{Coil2}$ represents the magnetic voltage source of both involved coils, where $\Theta_{Coil1} = i_1 N$ and $\Theta_{Coil2} = i_2 N$, with N as the number of windings. Θ_M represents the magnetic voltage source of the permanent magnets $\Theta_M = 2H_c h_m$, where H_c is the coercive field and h_m the thickness of the permanent magnets in direction of the magnetic flux Φ. The calculation of all magnetic resistances is based on the well-known reluctance equation

$$R_m = \frac{l_m}{\mu S}, \tag{3}$$

where l_m represents the length of the magnetic circuit, μ is its magnetic permeability and S represents the surface involved in the magnetic circuit. The reluctance of the iron parts, the coils and the air gaps are merged into single circuit elements (see Fig. 3). The leakage flux reluctance $R_{m\sigma}$ is derived from Finite-Element simulations. Solving the magnetic circuit leads to the magnetic fluxes through the circuit elements from which the magnetic flux density B_g in the air gap can be derived. One possibility to obtain the solution is the use of superposition. Therefore, only one magnetic voltage source is active at any time in order to calculate the magnetic fluxes within the network (Fig. 3). It is known that the superposition is applicable to linear systems only. Since nonlinear saturation effects are supposed to be implemented, a model based on superposition delivers correct results only for the linear range of the reluctance. Nevertheless, in order to involve nonlinear effects we designed an iterative equation system which determines linearized reluctance data for each magnetic flux calculation sequence.

2.3 The mechanical system

The mechanical model of the actuator is given by:

$$\ddot{x}(t) = \frac{F_L(t) - F_{fric}(t) + F_0(t)}{m}, \tag{4}$$

where $x(t)$ is the position of the armature. $F_{fric}(t) = k_d \dot{x}(t)$ is the friction force and $F_0(t)$ is the disturbance force acting on the armature. The mass of the armature is given by m. The Lorentz force $F_L(t) = l(i_1(t)B_{g1} + i_2(t)B_{g2})$ is determined by the electrical and by the magnetic system. Assuming quadratically shaped geometry boundaries as shown in Fig. 1, the scalar Lorentz force expression is applicable. Using superposition, the Lorentz force expression can be formulated as:

$$F_L(t) = \frac{2l}{A_{Coil}} \left(\frac{N(i_1^2(t) - i_2^2(t))}{R_{mRes1}} + g(t)(i_1(t) - i_2(t)) \right), \tag{5}$$

where R_{mRes1} is the magnetic resistance of the equivalent circuit (Fig. 3) with a short-cut voltage source Θ_M. A_{Coil} represents the coil area in flux direction. Expression $g(t)$ substitutes

$$g(t) = \left(\frac{R_{m\sigma}\Phi_{\sigma 2}}{R_{mAir} + R_{mCoil} + R_{mFeo}} \right), \tag{6}$$

where $\Phi_{\sigma 2}$ is the leakage flux generated by the permanent magnets. $g(t)$ is time varying since R_{mFeo} is subject to saturation effects. The presented system model was validated with finite-element programs. The modelling technique can be considered as a paradigm for similar actuator systems.

3 Problem statement

The nonlinear influence of term $N(i_1^2(t) - i_2^2(t))$ in Eq. (5) can be easily seen. It is obvious that this nonlinearity leads to problems of control. In this paper the following problem can be defined:

- To control state variables $i_1(t)$ and $i_2(t)$ so that $i_2(t) = -i_1(t)$.

In so doing, the nonlinear term $N(i_1^2(t) - i_2^2(t))$ in Eq. (5) is canceled. The electrical model part of the system described in Eq. (1) is linear and the following problem can be formulated.

Problem 1 (**Invariance**) *Given the system represented by Eq. (1), under the assumption $\mathbf{u}_q(t) = 0$ determine, if possible, a state feedback $\mathbf{u}(t) = \mathbf{Fi}(t)$ and an input partition matrix $\mathbf{S}_i$ such that,*

- *for state vector $\mathbf{i}(t)$ ($i_1(t)$ and $i_2(t)$), and two reference identical input functions $\mathbf{r}(t)$, the following relationship*

$$i_1(t) = -i_2(t) \tag{7}$$

holds.

□

Remark 1 *Condition (7) allows the cancellation of the nonlinearity of the actuator as stated in (5). The idea is to realize condition (7) as a permanent working condition of the actuator.* □

Given the dynamic system in Eq. (1) of a permanent magnetic actuator, and let

$$\mathbf{A} = \begin{bmatrix} -\frac{R_c}{L_{c1}L_{c5}} & \frac{R_cL_{c2}}{L_{c1}L_{c3}L_{c5}} \\ \frac{R_cL_{c4}}{L_{c1}L_{c3}L_{c5}} & -\frac{R_c}{L_{c3}L_{c1}} \end{bmatrix}; \tag{8}$$

$$\mathbf{B} = \begin{bmatrix} \frac{1}{L_{c1}L_{c5}} & -\frac{L_{c2}}{L_{c1}L_{c3}L_{c5}} \\ -\frac{L_{c4}}{L_{c1}L_{c3}L_{c5}} & \frac{1}{L_{c3}L_{c5}} \end{bmatrix}, \tag{9}$$

then a controller based on a state feedback gain $\mathbf{F}$ and an input partition matrix $\mathbf{S}_i$ which solve Problem 1. To be more precise, we look for an invariant and stabilizing state feedback matrix $\mathbf{F}$, along with input partition matrices $\mathbf{S}_i$ with $i = 1,2.$, such that, for the dynamic triples

$$(\mathbf{I}_i, \mathbf{A}+\mathbf{BF}, \mathbf{BS}_i), \tag{10}$$

the requirements

$$\mathscr{R}_{I_i} = \min\mathscr{I}(\mathbf{A}+\mathbf{BF}, \mathscr{B}\mathscr{S}_i) \subseteq \mathrm{im}\mathbf{I}_i \tag{11}$$

can be achieved. In Eq. (11), the following notations, as already indicated in the nomenclature section, $\mathscr{B} = \mathrm{im}\mathbf{B}$ and $\mathscr{S}_i = \mathrm{im}\mathbf{S}_i$ are used. In other words, we have to find the invariant controllable subspace $\mathscr{R}_{I_i}$ which depends on the actuator model parameters $\mathbf{A}$ and $\mathbf{B}$. For the currents $i_1(t)$ and $i_2(t)$ for instance, this subspace is a subspace of controllability [1] and it can be expressed by $\min\mathscr{I}(\mathbf{A}+\mathbf{BF}, \mathscr{B}\mathscr{S}_i)$.

[1]It is known that, $\min\mathscr{I}(\mathbf{A},\mathscr{B}) = \sum_{i=0}^{n-1}\mathbf{A}^i\mathrm{im}\mathbf{B}$ is the minimum $\mathbf{A}$–invariant subspace containing $\mathrm{im}(\mathbf{B})$.

This formulated criterion holds if the controlled subspace lies within the following subspace:

$$\mathbf{I}_i\mathscr{R}_{I_i} = \mathrm{im}\mathbf{I}_i. \tag{12}$$

In addition, the partition matrices $\mathbf{S}_i$ satisfy the following relationships

$$\mathrm{im}(\mathbf{BS}_i) \;=\; \mathrm{im}\mathbf{B}\cap\mathscr{R}_{I_i}. \tag{13}$$

Expression "im" of a matrix, e.g. $\mathrm{im}\mathbf{I}_i$ or $\mathrm{im}\mathbf{B}$, represents the image of that matrix which indicates the subspace created by the columns of this matrix. An invariant controllable subspace consists of state space vectors reachable through trajectories entirely lying in the subspace $\mathscr{R}_{I_i}$. Moreover, the trajectories lying in this subspace remain in this subspace.

4 Analysis of a procedure using a geometric approach based on a controlled invariant subspace

In [13] the authors proposed a decoupling control structure in order to achieve the cancelation of the nonlinearity stated by (5). Considering the following current subspaces:

$$\mathscr{C}_{i=1} = \mathscr{C}_{(1,0)} = \mathrm{im}\begin{bmatrix} 1 \\ 0 \end{bmatrix}, \tag{14}$$

$$\mathscr{C}_{i=2} = \mathscr{C}_{(0,1)} = \mathrm{im}\begin{bmatrix} 0 \\ 1 \end{bmatrix}. \tag{15}$$

In this approach, taking into account conditions (11) and (13), input partition matrices $\mathbf{S}_i$ can be determined by:

$$\mathbf{S}_{i=1} = \mathbf{S}_{(1,0)} = \begin{bmatrix} \frac{1}{L_{c1}L_{c5}} & -\frac{L_{c2}}{L_{c1}L_{c3}L_{c5}} \\ -\frac{L_{c4}}{L_{c1}L_{c3}L_{c5}} & \frac{1}{L_{c3}L_{c5}} \end{bmatrix}^{-1} \begin{bmatrix} 1 \\ 0 \end{bmatrix}, \tag{16}$$

$$\mathbf{S}_{i=1} = \mathbf{S}_{(1,0)} = \begin{bmatrix} L_{c1}^2\frac{L_{c3}L_{c5}}{L_{c1}L_{c3}-L_{c2}L_{c4}} \\ \frac{L_{c1}L_{c3}L_{c4}L_{c5}}{L_{c1}L_{c3}-L_{c2}L_{c4}} \end{bmatrix}. \tag{17}$$

To complete the calculation of the input partition matrix it follows:

$$\mathbf{S}_{i=2} = \mathbf{S}_{(0,1)} = \begin{bmatrix} \frac{1}{L_{c1}L_{c5}} & -\frac{L_{c2}}{L_{c1}L_{c3}L_{c5}} \\ -\frac{L_{c4}}{L_{c1}L_{c3}L_{c5}} & \frac{1}{L_{c3}L_{c5}} \end{bmatrix}^{-1} \begin{bmatrix} 0 \\ 1 \end{bmatrix}. \tag{18}$$

Through symbolic calculation the following result is obtained:

$$\mathbf{S}_{i=2} = \mathbf{S}_{(0,1)} = \begin{bmatrix} \frac{L_{c1}L_{c2}L_{c3}L_{c5}}{L_{c1}L_{c3}-L_{c2}L_{c4}} \\ L_{c3}^2 \frac{L_{c1}L_{c5}}{L_{c1}L_{c3}-L_{c2}L_{c4}} \end{bmatrix}. \quad (19)$$

In [13], in order to satisfy condition (11), matrix $\mathbf{F}$ must be designed such that:

$$\begin{bmatrix} -\frac{R_c}{L_{c1}L_{c5}} & \frac{R_cL_{c2}}{L_{c1}L_{c5}L_{c5}} \\ \frac{R_cL_{c4}}{L_{c1}L_{c3}L_{c5}} & -\frac{R_c}{L_{c3}L_{c1}} \end{bmatrix} + \begin{bmatrix} \frac{1}{L_{c1}L_{c5}} & -\frac{L_{c2}}{L_{c1}L_{c3}L_{c5}} \\ -\frac{L_{c4}}{L_{c1}L_{c3}L_{c5}} & \frac{1}{L_{c3}L_{c5}} \end{bmatrix} \mathbf{F} = \begin{bmatrix} \lambda & 0 \\ 0 & \lambda \end{bmatrix}. \quad (20)$$

In order to obtain $i_2(t) = -i_1(t)$ in Eq. (20) the two eigenvalues of the dynamics of the currents must be the same and this can be calculated by using matrix $\mathbf{F}$. Moreover, after that, the control system needs a proportional factor, which equals -1 in one of the inputs in order to obtain the required condition $i_2(t) = -i_1(t)$. Parameter λ represents the eigenvalues of the desired electrical system. For stability, λ must lie in the negative real plane. By adjusting the values of λ we can obtain a desired dynamics of the electrical system of the actuator which influences the whole dynamics of the actuator. After the cancelation due to the currents compensation, considering $i(t) = i_2(t) = -i_1(t)$ the following state variables can be chosen:

$$\mathbf{x}_f(t) = \begin{bmatrix} i(t) \\ y(t) \\ v(t) \end{bmatrix}, \quad (21)$$

where $y(t) = x(t)$ and $v(t) = \dot{x}(t)$, then the following matrices can represent the system:

$$\mathbf{A}_w = \begin{bmatrix} (-\frac{R_c}{L_{c1}L_{c5}} - \frac{R_cL_{c2}}{L_{c1}L_{c3}L_{c5}} + \frac{R_cL_{c4}}{L_{c1}L_{c3}L_{c5}} + \frac{R_c}{L_{c3}L_{c5}}) & 0 & 2lB_g \\ 0 & 0 & 1 \\ \frac{4lg}{A_{Coil}} & 0 & -\frac{k_d}{m} \end{bmatrix}, \quad (22)$$

$$\mathbf{B}_w = \begin{bmatrix} \frac{1}{L_{c1}L_{c5}} & -\frac{L_{c2}}{L_{c1}L_{c3}L_{c5}} \\ -\frac{L_{c4}}{L_{c1}L_{c3}L_{c5}} & \frac{1}{L_{c3}L_{c5}} \\ 0 & 0 \end{bmatrix}, \quad (23)$$

in which $g(t)$ is considered constant because of its small variability.

4.1 Speeding up the dynamics of the controlled system with the help of a geometric pre-compensator

In order to speed up the dynamics of the actuator without using strong actions of the regulators which can generate large oscillations and thus tracking errors, a geometric pre-compensator is proposed. The idea is to select an eigenvector of matrix $\mathbf{A}_W$ which represents the matrix of the predicted dynamics of the whole actuator. This eigenvector must be included in the intersection between $\mathsf{im}\mathbf{B}_W$ and between the set of the eigenvectors of matrix $\mathbf{A}_W$. Once the eigenvector which corresponds to the biggest absolute value of the eigenvalue is chosen, according to the meaning of the eigenvalues and eigenvectors, then it is possible to control the system along the direction of this eigenvector to obtain the fastest dynamics. The advantage here is that these dynamics can be reached using just another input partition matrix which should select the eigenvector of the system. If a matrix $\mathbf{I}_\lambda$ is considered, such that:

$$\mathsf{im}\mathbf{I}_\lambda = \{\mathsf{im}\mathbf{B}_W \cap \mathsf{im}\mathbf{V}_W\}, \quad (24)$$

where $\mathbf{V}_W$ represents the matrix containing all eigenvectors of matrix $\mathbf{A}_W$, then subspace $\mathsf{im}\mathbf{I}_\lambda$ represents the intersection subspace between the image of the matrix of the eigenvectors and the image of input matrix $\mathbf{B}_W$. Considering $\mathbf{I}_{\lambda_{max}}$ which represents the eigenvector of set defined in (24) to which the maximal absolute value of an eigenvalue corresponds, then we are looking for an input partition matrix $\mathbf{S}_p$ such that, for the dynamic triples

$$\left(\mathbf{I}_{\lambda_{max}}, \mathbf{A}_W, \mathbf{B}_W\mathbf{S}_p\right), \quad (25)$$

the requirements

$$\mathscr{R}_{I_i} = \min \mathscr{I}(\mathbf{A}_W, \mathscr{B}_W\mathscr{S}_p) \subseteq \mathsf{im}\mathbf{I}_{\lambda_{max}} \quad (26)$$

can be achieved. In Eq. (26), the following notations, as already indicated in the nomenclature section, $\mathscr{B}_W = \mathsf{im}\mathbf{B}_W$ and $\mathscr{S}_p = \mathsf{im}\mathbf{S}_p$ are used. About the calculation of input partition matrix $\mathbf{S}_p$, if $\mathsf{im}\mathbf{B}_W \cap \mathsf{im}\mathbf{V}_W \neq 0$, then:

$$\mathbf{S}_p = (\mathbf{B}_W^T\mathbf{B}_W)^{-1}\mathbf{B}_W^T\mathbf{I}_{\lambda_{max}}. \quad (27)$$

5 Solving a linear position MPC optimization problem

Considering the models described by the matrices in (22) and (23) in which Euler discretization is considered with $k = nT_s$, $n \in \mathbb{N}$, where T_s is the sampling time. If $y(t) = x(t)$ is the position of the actuator which is assumed to be the controlled output, and $v(t) = \dot{x}(t)$, then a control structure is obtained similar to that presented in [21]. This contribution proposes an advancement of the work in [21]. In fact, a pre-selection matrix S_{wk} which, as already explained, is calculated using the eigenvectors of the mechanical model, and is included in the proposed MPC algorithm to speed up the dynamic performances. The following system is proposed:

$$\begin{aligned} \mathbf{x}_f(k+1) &= \mathbf{A}_{wk}\mathbf{x}_f(k) + \mathbf{B}_{wk}\mathbf{S}_p \begin{bmatrix} u_1(k) \\ u_2(k) \end{bmatrix} \\ y(k) &= \mathbf{H}_k\mathbf{x}_f(k), \end{aligned} \tag{28}$$

where

$$\mathbf{x}_f(k) = \begin{bmatrix} i(k) \\ y(k) \\ v(k) \end{bmatrix} \tag{29}$$

and matrix $\mathbf{H}_k = [0 \quad 1 \quad 0]$ is the output matrix which determines the position of the valve according to the whole system represented by matrix $\mathbf{A}_{wk}$. In MPC approach just two samples are considered:

$$y(k+1/k) = \mathbf{H}_k\mathbf{A}_{wk}\mathbf{x}_f(k) + \mathbf{H}_k\mathbf{B}_{wk}\mathbf{S}_p u_{mpc}(k) \tag{30}$$

$$\begin{aligned} y(k+2/k) = \mathbf{H}_k\mathbf{A}_{wk}^2\mathbf{x}_f(k) + \mathbf{H}_k\mathbf{A}_{wk}\mathbf{B}_{wk}\mathbf{S}_p u_{mpc}(k) + \\ \mathbf{H}_k\mathbf{B}_{wk}\mathbf{S}_p u_{mpc}(k+1). \end{aligned} \tag{31}$$

Eqs. (30) and (31) can be vectorially expressed as:

$$\mathbf{Y}(k) = \mathbf{G}_p\mathbf{x}_f(k) + \mathbf{F}_{1p}(k)\mathbf{U}_{mpc}(k), \tag{32}$$

where

$$\mathbf{U}_{mpc}(k) = \begin{bmatrix} u_{mpc}(k) & u_{mpc}(k+1) \end{bmatrix}, \tag{33}$$

and

$$\mathbf{F}_{1p} = \begin{bmatrix} \mathbf{H}_k\mathbf{B}_{wk}\mathbf{S}_p & \mathbf{0} \\ \mathbf{H}_k\mathbf{A}_{wk}\mathbf{B}_{wk}\mathbf{S}_p & \mathbf{H}_k\mathbf{B}_{wk}\mathbf{S}_p \end{bmatrix}, \tag{34}$$

$$\mathbf{G}_p = \begin{bmatrix} \mathbf{H}_k\mathbf{A}_{wk} \\ \mathbf{H}_k\mathbf{A}_{wk}^2 \end{bmatrix}. \tag{35}$$

If the following performance criterion is assumed,

$$\begin{aligned} J = \frac{1}{2}\sum_{j=1}^{N}\Big(y_d(k+j) - y(k+j)\Big)^{\mathrm{T}}\mathbf{Q}_p \times \\ \Big(y_d(k+j)) - y(k+j)\Big) + \\ \frac{1}{2}\sum_{j=1}^{N}\Big(u_{mpc}(k+j)\Big)^{\mathrm{T}}\mathbf{R}_p u_{mpc}(k+j), \end{aligned} \tag{36}$$

where $y_d(k+j)$, $j = 1, 2, \ldots, N$ is the position reference trajectory (desired trajectory) and N the number of samples of the prediction horizon, and $\mathbf{Q}_p$ and $\mathbf{R}_p$ are non-negative definite matrices, then the solution minimizing performance index (36) may then be obtained by solving

$$\frac{\partial J}{\partial u_{mpc}(k)} = 0. \tag{37}$$

A direct off-line computation may be obtained explicitly as:

$$\begin{aligned} u_{mpc}(k) = (\mathbf{F}_{1p}^{\mathrm{T}}\mathbf{Q}_p\mathbf{F}_{1p} + \mathbf{R}_p)^{-1}\mathbf{F}_{1p}^{\mathrm{T}}\mathbf{Q}_p \times \\ \Big(\mathbf{Y}_{d_p}(k) - \mathbf{G}_p\mathbf{x}_f(k)\Big), \end{aligned} \tag{38}$$

where $\mathbf{Y}_{d_p}(k)$ and $\mathbf{Y}_p(k)$ are the desired output column vector and the measured or observed output vector. For further details on this optimization procedure see [23].

6 Simulation results

The presented case considers an actuator of $21kg$ as a moving mass. The mass must be moved to reach a position of $8mm$ with respect to the initial one. In the shown simulations, a sampling time T_s equals 0.1ms is used. In Fig. 4 the block diagram of the whole control system is shown. The computer simulations were done using Matlab/Simulink developed by MathWorks. Matlab routines which realise the controller are integrated with Simulink being used to represent and simulate the actuator. **Case 1, Figs. 5 and 6:** Simulations with the controller stated by matrices $\mathbf{F}$ and $\mathbf{S}_i$ but without pre-compensation matrix $\mathbf{S}_p$. In Fig. 5 input voltages and current coils simulation using the control scheme without using the eigenvector structure is shown. Figures 5 and 6 show simulation results using the decoupling geometric structures $\mathbf{F}$ and $\mathbf{S}_i$ which satisfy conditions of Eqs. (11), (12) and (13) but without using the pre-compensator stated in Eq. (27). In particular, from Fig. 5 it is possible to observe that the coil currents are oscillating ones. In Fig. 6 the effects of the signals of Fig. 5 on the position and on the velocity of the actuator are shown. In more detail, on the upper part part of Fig. 6 the effect on a test positioning is shown. It is possible to see how, in case pre-compensation matrix $\mathbf{S}_p$ of Eq. (27) is not used, overshoot and oscillations of the response to the step function are present. **Case 2;**

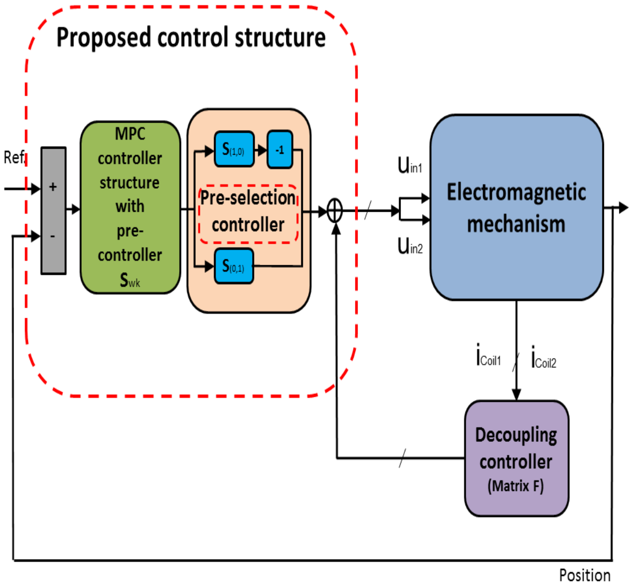

Figure 4: Block diagram of the whole control system

Figs. 7 and 8: Simulations with the controller stated by matrices $\mathbf{F}$, $\mathbf{S}_i$ and with pre-compensation matrix $\mathbf{S}_p$. In Fig. 7 the simulation results of the proposed approach are shown. Figure 7 shows the input voltage coils (the upper part of the figure) and the compensated coil currents (the lower part of the figure) using the decoupling geometric structures $\mathbf{F}$ and $\mathbf{S}_i$ which satisfy conditions of Eqs. (11), (12) and (13) and using the pre-compensator stated in Eq. (27). In the simulations of Figs. 7 and 8 the same matrices $\mathbf{F}$ and $\mathbf{S}_i$ as in **Case 1** are proposed. Figure 8 shows the effects of the signals of Fig. 7 on the position and on the velocity of the actuator. In more detail, on the upper part of Fig. 8 the effect on a test positioning is shown. It is possible to see how, by using pre-compensation matrix $\mathbf{S}_p$ of Eq. (27), the overshoot and oscillations are not present on the response to the step function. In both analyzed cases, **Case 1** and **Case 2**, matrices $\mathbf{Q}_p$ and $\mathbf{R}_p$ are set such that the energy needed to achieve the desired position within 0.1s is the same.

7 Conclusions

The paper deals with a control for a permanent magnetic actuator. The controller is designed in order to cancel the nonlinearity of the proposed actuator. The proposed approach uses the invariant subspace theory. After cancelling the nonlinearity, a pre-compensation action is used to speed up the controlled dynamics of

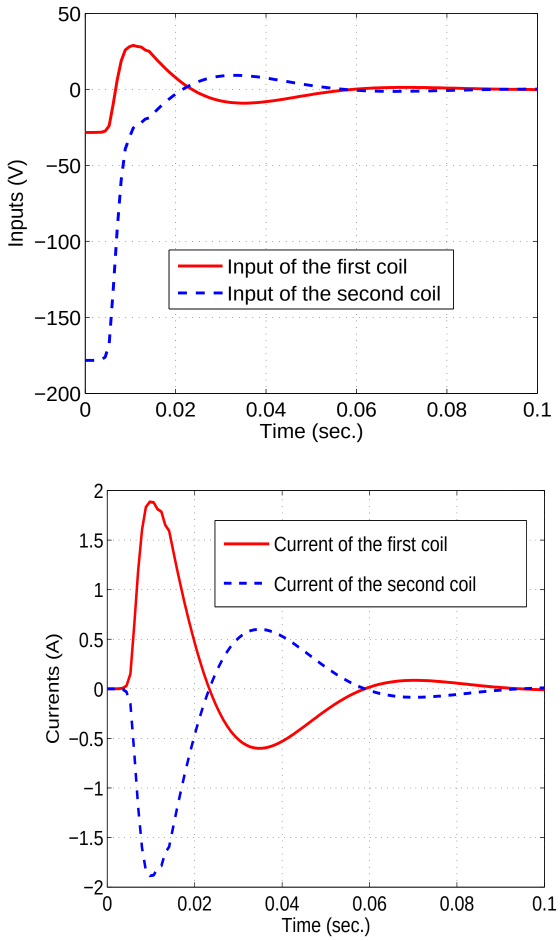

Figure 5: Top: Inputs voltage $u_1(t)$ and $u_2(t)$ of the coils. Bottom: Current $i_1(t)$ and $i_2(t)$ in the coils of the actuator.

the actuator and a linear MPC strategy is applied for the control of the positioning. The advantage of this proposed method is that the control structure is a very simple one which is based on the concept of the invariant subspaces to cancel the nonlinearity. The main disadvantage is that the cancellation method can be imperfect and thus the linearization can be flawed. A possible improvement could be to implement a robust decoupling control law as mentioned in the introduction.

Acknowledgements: Particular thanks are directed to Steffen Braune of the IAI (Institute for Automation and Informatics), Wernigerode (Germany) and to Kai Lehman for their work and time they spent in IAI for technical support. This work would not have been accomplished without them.

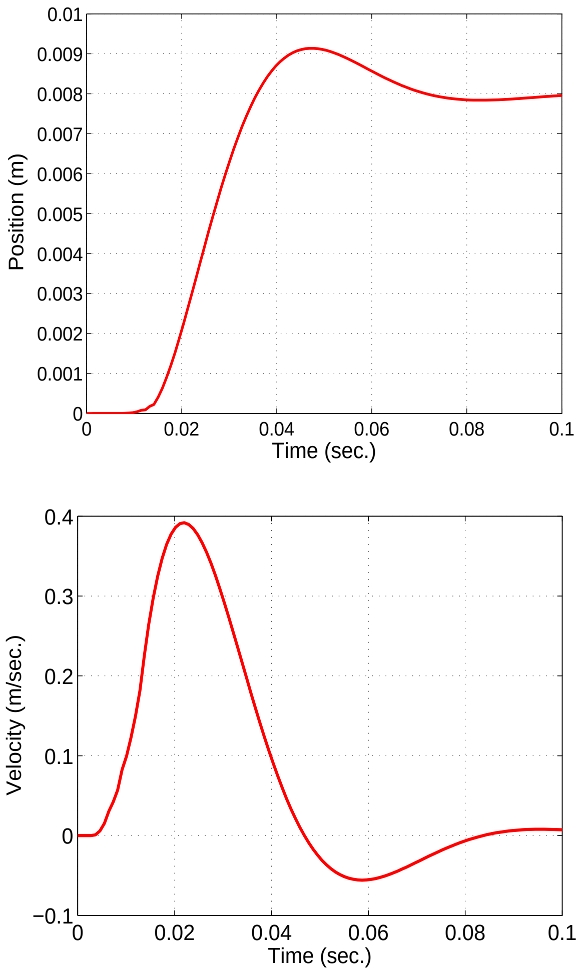

Figure 6: Top: Position of the actuator. Bottom: Velocity of the actuator.

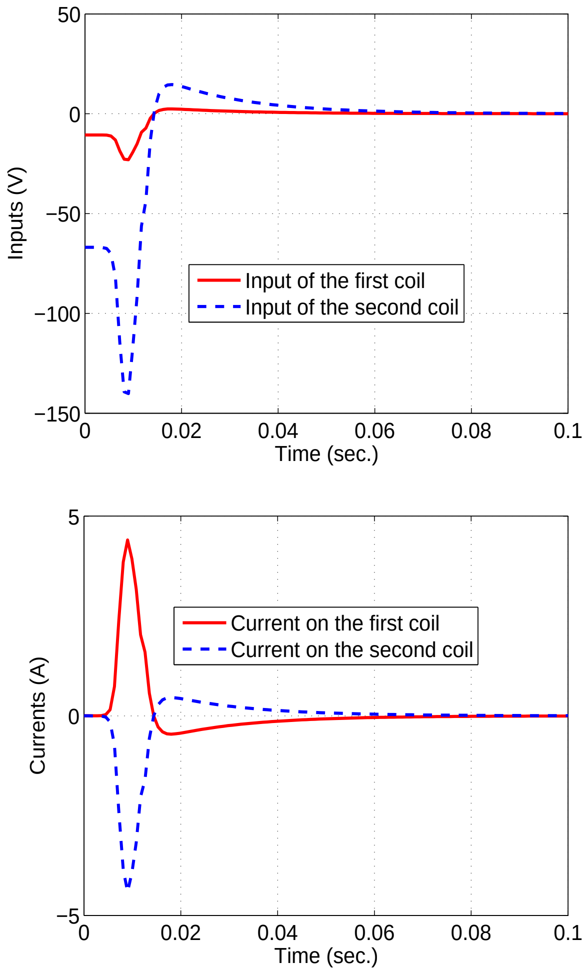

Figure 7: Top: Inputs voltage $u_1(t)$ and $u_2(t)$ of the coils using the proposed method. Bottom: Current $I_1(t)$ and $I_2(t)$ in the coils of the actuator using the proposed method.

References:

[1] Basile G, Marro G (1992) Controlled and conditioned invariants in linear system theory. Prentice Hall, New Jersey-USA

[2] Isidori A (1989) Nonlinear Control Systems. Springer-Verlag, Heidelberg

[3] Wonham W.M (1979) Linear multivariable control: a geometric approach. Springer-Verlag, New York

[4] Bhattacharyya S.P (1983) Generalized controllability, controlled invariant subspace and parameter invariant control. SIAM Journal on Algebraic Discrete Methods 4(4):529–533

[5] Marro G, Barbagli F (1999) The Algebraic Output Feedback in the Light of Dual-Lattice Structures. Kybernetika 35(6):693–706

[6] Prattichizzo D, Mercorelli P (2000) On some geometric control properties of active suspension systems. Kybernetika 36(5):549–570

[7] Mercorelli P (2010) Robust decoupling through algebraic output feedback in manipulation systems. Kybernetika 46(5):850–869

[8] Mercorelli P (2010) Geometric Structures for the Parameterization of Non-interacting Dynamics for Multi-body Mechanisms. International Journal of Pure and Applied Mathematics-IJPAM 59(3):257–273

[9] Mercorelli P (2012) Decoupling dynamic regulator with a minimum variance error estimator for online parameters indentification of permanent magnet three-phase synchronous motors.

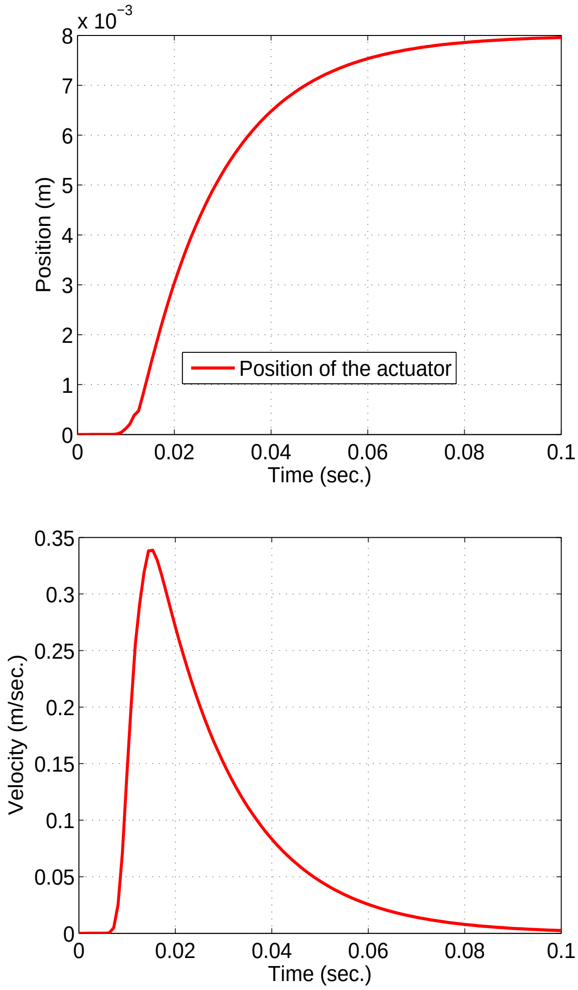

Figure 8: Top: Position of the actuator using the proposed method. Bottom: Velocity of the actuator using the proposed method.

In: Proceedings of the 16th IFAC Symposium on System Identification, pages 757–762, Brussels

[10] Mercorelli P (2012) A two-stage augmented extended Kalman filter as an observer for sensorless valve control in camless internal combustion engines. IEEE Transactions on Industrial Electronics 59(11):4236–4247

[11] Mercorelli P (2012) A hysteresis hybrid extended Kalman filter as an observer for sensorless valve control in camless internal combustion engines. IEEE Transactions on Industry Applications 48(6):1940–1949

[12] Mercorelli P (2012) A trajectory generation algorithm for optimal consumption in electromagnetic actuators. IEEE Transactions on Control Systems Technology, 20(4):1025–1032

[13] Mercorelli P, Lehmann K, Liu S (2003) On robustness properties in permanent magnet machine control using decoupling controller. In: Proceedings of the 4^{th} IFAC International Symposium on Robust Control Design, ROCOND '03, Milan

[14] Mercorelli P (2012) On the nonlinearity compensation in permanent magnet machine using a controller based on a controlled invariant subspace. Procedia Engineering a journal of Elsevier Science 50:592–600

[15] Qin S.J, Badgwell T.A. (2003) A survey of industrial model predictive control technology. Control Engineering Practice, 11(7):733-764

[16] Siller-Alcala I.I, Abderrahim M, Jaimes-Ponce J, Alcantara-Ramirez R (2008) Speed-Sensorless Nonlinear Predictive Control of a Squirrel Cage Motor. WSEAS Transactions on Systems and Control 3(2):99–104

[17] Kassem A.M (2012) Predictive Voltage Control of Stand Alone Wind Energy Conversion System. WSEAS Transactions on Systems and Control 7(3):97–107

[18] Yousef A.M (2012) Model Predictive Control Approach Based Load Frequency Controller. WSEAS Transactions on Systems and Control 6(7):265–275

[19] Wei Y, Xiuqiong H, Juan Y, Wenyuan L (2011) A Preventive Control Model for Static Voltage Stability and Thermal Stability based on Power Transfer Capabilities of Weak Branches. WSEAS Transactions on Circuits and Systems 10(5):147–156

[20] Hu Z, Farson D.F (2008) Design of a waveform tracking system for a piezoelectric actuator. In: Proceedings of the Inst. Mech. Eng., J. Syst. Control Eng. 222: 11-21.

[21] Mercorelli P (2012) A switching Kalman filter for sensorless control of a hybrid hydraulic piezo actuator using mpc for camless internal combustion engines. In: Proceedings of the 2012 IEEE International Conference on Control Applications, pages 980–985, Dubrovnik

[22] Mercorelli P (2012) An anti-saturating adaptive pre-action and a slide surface to achieve soft landing control for electromagnetic actuators. IEEE/ASME Transactions on Mechatronics 17(1):76–85

[23] Huang S, Kiong T.K, Lee T.H (2002) Applied Predictive Control. Springer-Verlag, London